colorants

MDPI

Article

Azaphilones Pigments from the Fungus *Penicillium hirayamae*

Coralie Pavesi [1], Victor Flon [2], Grégory Genta-Jouve [3], Elodie Pramil [4], Alexandre Escargueil [4], Adeel Nasir [5], Tristan Montier [5,6], Xavier Franck [2,*] and Soizic Prado [1,*]

1 Muséum National d'Histoire Naturelle, Unité Molécules de Communication et Adaptation des Micro-Organismes, UMR 7245, CP 54, 57 rue Cuvier, 75005 Paris, France
2 Normandie Université, CNRS, UNIROUEN, INSA Rouen, COBRA (UMR 6014 & FR 3038), 76000 Rouen, France
3 UAR3456 CNRS LEEISA, Laboratoire Ecologie, Evolution, Interactions des Systèmes Amazoniens, Centre de Recherche de Montabo, IRD, 275 Route de Montabo, CEDEX BP 70620, 97334 Cayenne, France
4 Sorbonne University INSERM U938, Centre de Recherche Saint-Antoine, 75012 Paris, France
5 Brest University, INSERM, Etablissement Français du Sang, Unité Génétique Génomique Fonctionnelle et Biotechnologie, UMR 1078, 29200 Brest, France
6 Centre Hospitalier Régional Universitaire de Brest, Service de Génétique Médicale et de Biologie de la Reproduction, Centre de Référence des Maladies Rares "Maladies Neuromusculaires", 29200 Brest, France
* Correspondence: xavier.franck@insa-rouen.fr (X.F.); soizic.prado@mnhn.fr (S.P.)

Abstract: The use of fungal pigments as dyes is attractive for various industries. Fungal pigments arise a strong interest because they are suitable for large-scale industrial production and have none of the drawbacks of synthetic pigments. Their advantages over synthetic or vegetal dyes mark them as a prime target. Azaphilones are fungal polyketides pigments bearing a highly oxygenated pyranoquinone bicyclic core produced by numerous species of ascomyceteous and basidiomyceteous fungi. In order to find new azaphilones dyes, the fungal strain *Penicillium hirayamae U.*, a known producer of azaphilone but, chemically, barely studied so far, was investigated by molecular networking and led to the isolation of three new azaphilones, penazaphilone J-L, along with the known penazaphilone D, isochromophilone VI, and sclerketide E. Their structures were determined based on extensive NMR and the absolute configurations by ECD. All compounds were evaluated for their cytotoxic activity against human cell lines and human pathogenic-resistant strains.

Keywords: azaphilone; pigment; cytotoxicity

Citation: Pavesi, C.; Flon, V.; Genta-Jouve, G.; Pramil, E.; Escargueil, A.; Nasir, A.; Montier, T.; Franck, X.; Prado, S. Azaphilones Pigments from the Fungus *Penicillium hirayamae*. *Colorants* **2023**, *2*, 31–41. https://doi.org/10.3390/colorants2010003

Academic Editor: Anthony Harriman

Received: 25 November 2022
Revised: 6 January 2023
Accepted: 18 January 2023
Published: 25 January 2023

1. Introduction

Fungal pigments are of great interest to food colorant industries because they are suitable for large-scale industrial production and do not have the disadvantages of synthetic pigments. Fungal pigments have the advantage of being produced using sources of carbon and nitrogen, which can even be obtained from food by-products or from agro-industrial waste. Moreover, public awareness of the adverse effects of synthetic dye increased the demand for natural pigments, even though only 25 natural colorants are approved by the European Union so far [1].

Azaphilones are fungal polyketides pigments bearing a highly oxygenated pyranoquinone bicyclic core produced by numerous species of ascomyceteous and basidiomyceteous fungi [2]. In Asia, *Monascus*-fermented rice is used to produce azaphilone pigments for centuries. Azaphilones are one of the most promising classes of fungal pigments in research as industrial pigments, especially because they stand out for their yellow, orange, and red colors. Thus, they received an increasingly great deal of research interest, especially for their applications in the dyeing, cosmetic, and printing industries [3–5].

In the search for new azaphilone pigments produced by fungi, we used molecular networking and the latest Sirius 5.5.5 version for fungal metabolites annotation in order to efficiently identify the presence of azaphilones in fungal extracts and optimize the search

for new ones. Using this approach, we identified the fungus *Penicillium hirayamae* as a producer of novel azaphilones. Three new azaphilones named penazaphilones J-L (**1**–**3**), along with three known ones, penazaphilone D, isochromophilone VI, and sclerketide E [6–8] were isolated and identified from the ethyl acetate extract of the solid culture of the strain *Penicillium hirayamae*. Here, the isolation, structure elucidation, and biological activities of these compounds were described.

2. Materials and Methods

2.1. General Experimental Procedures

Optical rotations $[\alpha]^{20}_{D}$ were determined using an Anton Paar MCP 150 polarimeter. IR spectra were performed on a PerkinElmer BX FR-IR spectrometer, and CD spectra finished Jasco J-810 spectropolarimeter system. UV spectra were recorded on Uvikon 9 X 3 W Bioserv. High-resolution mass spectra were recorded on a Maxis IITM QTOF mass spectrometer (Bruker, Billerica, MA, USA) with an electrospray ionization source.

^{1}D and ^{2}D NMR spectra were recorded on Avance III HD 400 MHz and 600 MHz spectrometers (Bruker, Wissembourg, France) equipped with a BBFO Plus Smart probe and a triple resonance TCI cryoprobe, respectively (CNRS-MNHN).

Preparative HPLC experiments were performed on an Agilent system and an Agilent (Santa Clara, CA, USA) PrepHT XDB-C18 column (21.2 × 150 mm i.d.; 5 µm; USA). Column chromatography (CC) was performed using 200 g of silica gel (Geduran Si 60, 40−63 µm, Merck, Darmstadt, Germany and Lichroprep RP-18, 40–63 µm, Merck KGaA).

The HPLC-MS/MS data were obtained with the C18 AcclaimTM RSLC PolarAdvantage II column (2.1 × 100 mm, 2.2 µm of pore size; Thermo Fisher Scientific, Massachusetts, USA) connected to a Dionex Ultimate 3000 HPLC system and coupled to a Maxis IITM QTOF mass spectrometer (Bruker, Wissembourg, France) with an electrospray ionization source. The mobile phases were water (0.1% formic acid, solvent A) and acetonitrile (0.08% formic acid, solvent B) following a gradient of B at 10–100 in 15 min. The flow rate was set at 300 µL min^{-1}. The MS parameters were 3.5 kV of electrospray voltage, 35 psi of nebulizing gas (N_2) pressure, drying gas (N_2) flow rate of 8 L min^{-1}, and 200 °C of drying temperature.

The LC-MS/MS data were preprocessed on Mzmine 2.53 with a noise level of 9.0E2 for MS1 and 1.0E1 for MS2, the ADAP chromatogram built with a minimum group size of a scan of 5, a group intensity threshold and minimum highest intensity at 1.0E1. The data were then deisotoped and filtered to only keep peaks with MS2 scans. The data were then exported on FBMN-GNPS to build a molecular network with a cosine of 0.5 and 3 minimum matched fragment ions. The precursor ion mass tolerance (PIMT) and fragment ion mass tolerance (FIMT) were at 0.02 Da.

2.2. Fungal Materials

The strain of *Penicillium hirayamae* was purchased from CBS-KNAW fungal collection (CBS number 229.60). Precultures were obtained by seeding 3 cubes of agar covered with the mycelium of *P. hirayamae* and incubated for 8 days at 25 °C. The medium used for the preculture was the following: 40 g of sucrose, 5 g of yeast extract, 10 g of peptone, and 10 g of agar for 1 L of distilled water. Precultures were then scratched and sprayed with 100 mL of sterilized water, 1 mL of the mix was thus spread on 100 Petri dishes and at 25 °C for 10 days. The medium used for the culture was the same as for the preculture.

2.3. Extraction and Isolation

The content of the 100 Petri dishes was cut into cubes and extracted three times with ethyl acetate by sonication (30 min each time). The solvent was evaporated under reduced pressure to give a crude extract of 4.64 g, which was fractionated over a silica gel column (100 g) and eluted successively with dichloromethane/ethyl acetate (9:1) and dichloromethane/methanol (8:2) to afford 6 fractions.

The fraction 6 (2.555 g) was purified by preparative HPLC (10 mL/min, A: water + 0.1% formic acid, B: acetonitrile, gradient: from 5 to 50% of B for 4 min, then from 50 to 95% of

B during 26 min) yielding 11 fractions. The subfraction F6F10 (15.4 mg) was the new penazaphilone J. The subfraction F6F6 was submitted to preparative TLC (dichloromethane/methanol, 9:1) to yield the subfraction F6F6F1 (1.5 mg) corresponding to the penazaphilone L. The subfraction F6F3 (21.2 mg) was purified by a second preparative HPLC (10 mL/min, A: water + 0.1% formic acid, B: acetonitrile, gradient: from 5 to 55% of B for 2 min, then from 55 to 95% of B for 16 min) yielding penazaphilone D (1.8 mg), isochromophilone VI (2 mg) and sclerketide E (7.2 mg).

The fraction 4 (806 mg) was purified by preparative HPLC (10 mL/min, A: water + 0.1% formic acid, B: acetonitrile, gradient: from 5 to 40% of B for 4 min, then from 40 to 95% of B during 26 min) yielding 11 fractions.

Purification of the subfraction F4F7 by preparative HPLC (5 mL/min, A: water + 0.1% formic acid, B: methanol, gradient: from 5 to 70% of B for 4 min, from 70 to 80% of B for 20 min then from 80 to 90% of B for 22 min) afforded the subfraction F4F7F2 (1.1 mg) named penazaphilone K.

*2.4. Penazaphilone J (**1**)*

Red amorphous powder, $[\alpha]^{20}{}_{D}$ -142 (*c* 0.04, MeOH); UV (CH_3OH) λmax: (log ε) 372 (3.1) nm; IR ν_{max} (thin film) cm^{-1}: 2100, 1643; ^{1}H NMR (600 MHz, CD_3CN) see Table 1; ^{13}C NMR (600 MHz, CD_3CN) see Table 1; ESI-MS *m/z*: 460.2253 $[M+H]^+$.

*2.5. Penazaphilone K (**2**)*

Red amorphous powder, $[\alpha]^{20}{}_{D}$ -10 (*c* 0.2, MeOH); UV (CH_3OH) λmax: (log ε) 354 (187) nm; IR ν_{max} (thin film) cm^{-1}: 3412, 2094, 1641; ^{1}H NMR (600 MHz, DMSO-d_6) see Table 1; ^{13}C NMR (600 MHz, DMSO-d_6) see Table 1; ESI-MS *m/z*: 510.2057 $[M+H]^+$.

*2.6. Penazaphilone L (**3**)*

Red amorphous powder, $[\alpha]$ $^{20}{}_{D}$ -34 (*c* 0.15, MeOH); UV (CH_3OH) λmax: (log ε) 371 (3.3) nm; IR ν_{max} (thin film) cm^{-1}: 3437, 2931, 2343, 1703, 1587,1252; ^{1}H NMR (600 MHz, CD_3CN) see Table 1; ^{13}C NMR (600 MHz, CD_3CN) see Table 1; ESI-MS *m/z*: 891.3401 $[M+H]^+$.

2.7. Computational Details

DFT calculations have been performed using Gaussian 16 W [9]. Prior to geometry optimization, all compounds were submitted to a conformational analysis using the GMMX package with the MMFF94 forcefield (energy threshold = 1 kcal/mol). After geometry optimization and frequency calculation at the b3lyp/6–31g(d) level. ECD spectra were plotted using GaussView 6.

2.8. Biological Activities

2.8.1. Cytotoxic Activities

HCEC-1CT human colon epithelial cell line was purchased from Evercyte and maintained in DMEM (Gibco) in addition with cosmic calf serum (2%), EGF (20 ng/mL), Insulin (10 µg/mL), Apo-Transferrin (2 µg/mL), sodium-selenit (5 nM) and Hydrocortisone (1 µg/mL). Cell viability was assessed by CellTiter Glo 2.0 Luminescent Viability assay (Promega). At J0, 2500 cells were seeded in a white 96-well plate in a final volume of 100 µL. At J1, cells were treated with compounds (**1**–**3**) at the indicated concentrations (final concentration obtained by serial dilutions from 100 µg/mL to 1.56 µg/mL in DMSO 1%). At J2, the plate and CellTiter Glo 2.0 reagent are equilibrated to room temperature for 20 min, and 100 µL of CellTiter Glo 2.0 reagent was added to each well. The plate is agitated for 2 min on an orbital shaker and then incubated at room temperature for 10 min. Mono-oxygenation of luciferin is catalyzed by luciferase in the presence of ATP, liberated by viable cells. Luminescence was measured in a microplate reader, Infinite 200Pro (TECAN), as described by Dillard et al. [10]. The results are expressed as a ratio compared to the

control using the following formula: Pourcentage = 100 × [(compounds lum)/(control lum)]. All values are averages of three experiments performed in triplicate.

Compounds (**1**–**3**) were also evaluated against A549 and 16HBE cell lines, adenocarcinomic human alveolar basal epithelial cell line and human bronchial epithelial cell lines, respectively. Briefly, A549 cells were seeded in a 96-well plate at 1.5×10^4 cells/well with 100 µL DMEM cell culture media. In total, 16 HBE cells were seeded in a 96-well plate at 4×10^4 cells/well with 100 µL MEM cell culture media. Both cell lines were cultivated overnight into a humified incubator (37 °C and 5% of CO_2) for cell growth. On day 2, half of the cell culture media (50 µL) was removed from the plate and replaced with the same volume of fresh cell culture media containing various concentrations of the compounds (**1**–**3**, final concentration obtained by serial dilutions from 100 µg/mL to 1.56 µg/mL in DMSO 1%) and various concentrations of DMSO as solvent control (serial dilution from 10% to 0.1%) and cells alone as the negative control. On day 3, cell viability was carried out by two types of assays, ViaLight and ToxiLight-LONZA, based on luminescence measurement (Vialight and Toxilight). All values are averages of three experiments performed in triplicate.

2.8.2. Antimicrobial Assay

The antimicrobial effects of **1**, **2,** and **3** were evaluated on human pathogenic gram-negative and positive bacteria, Pseudomonas aeruginosa and Staphylococcus aureus, respectively, as reported earlier [11–13]. The methicillin-resistant clinical strain of S. aureus, N315 (13), and the multidrug-resistant clinical strain of P. aeruginosa, PAH [11] were used in the assay. Briefly, DMSO-dissolved azaphilones pigments were diluted in 50 µL of Luria broth (LB) media and transferred to a 96-well transparent plate. Subsequently, the volume was made up to 100 µL by adding 50 µL of bacterial culture in LB media to achieve bacterial cell numbers of 7.5×10^5 CFU/mL. The bacterial inoculum used for the assay was obtained from an overnight-grown pre-culture of the respective strains. After 24 h of growth (37 °C, at constant shaking), the optical density (OD) at an absorbance of 600 nm of treated and non-treated samples was evaluated using the multiple-reader Mithras2 LB 943 (Berthold Technology, Thoiry, France). In addition, 5 µL from each well of the 96-well plate was transferred to a solid LB agar plate. The following day, the overnight incubated (37 °C) LB agar plate was monitored for the antimicrobial effects of azaphilones, and an image was acquired.

3. Results

Penicillium hirayamae Udagawa (CBS 229.60) was discovered by S. Udagawa in 1959 and has been little studied so far [14]. Indeed, only three metabolites were described from this species, the azaphilones (-) sclerotiorin, (-) sclerotioramine, and rubrorotiorin [15,16]. From the holotype *Eupenicillium hirayamae* D.B. Scott & Stolk, only the secondary metabolite desoxyverrucarin E was described [17]. Accordingly, in order to isolate new azaphilones from fungi, *Penicillium hirayamae* U. was purchased, and its crude extract was analyzed by molecular network. This latter pointed out a specific cluster of azaphilones. Indeed, combined annotations from GNPS databases and SIRIUS version 5.5.5 highlighted the presence of various ions identified as azaphilones (Figure 1). Among the annotated azaphilones, penazaphilone D [8], isochromophilone VI [7], and sclerketide E [6] were fully chemically characterized by 2D NMR after isolation from the *Penicillium hirayamae* crude extract, reinforcing the GNPS and SIRIUS predictions. Among the known compounds produced by *P. hirayamae*, only the sclerotiorin was identified from GNPS and Sirius (Figure S1).

Non-identified ions of the cluster were thus targeted for the next isolation steps, which led to the isolation of three new azaphilones named penazaphilone J-L (**1**–**3**) (green nodes, Figure 1). It is noteworthy that grey nodes represent azaphilones present in too small quantities in the extract to be isolated in sufficient amounts and fully elucidated.

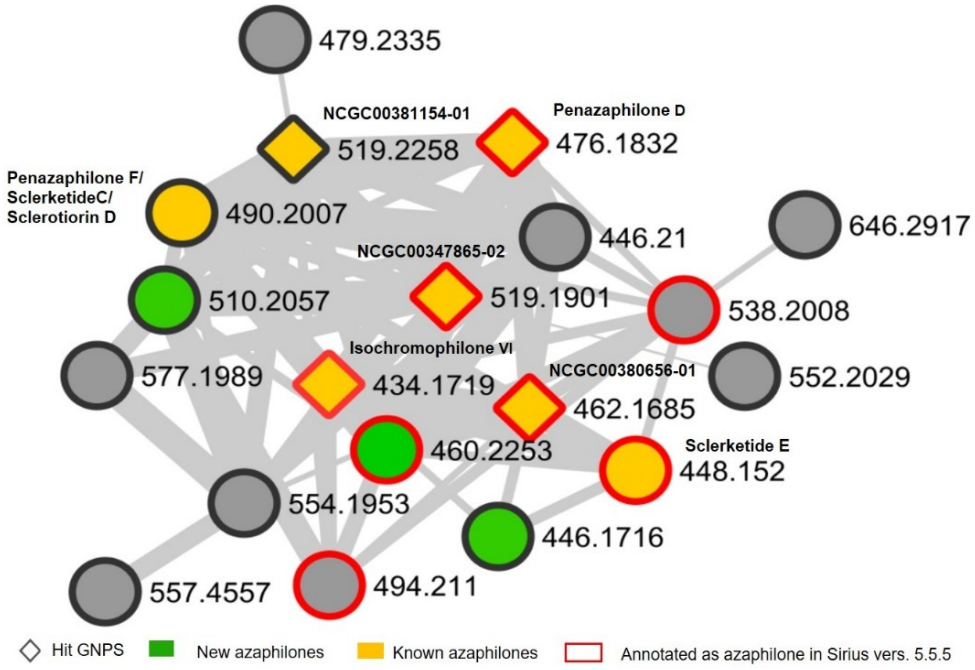

Figure 1. Cluster of azaphilones obtained from the molecular network of *P. hirayamae* crude extract and annotated by GNPS databases and Sirius vers. 5.5.5.

Penazaphilone J (**1**) was obtained as a red amorphous powder and assigned a molecular formula of $C_{26}H_{34}ClNO_4$ based on the HRESIMS peak at *m/z* 460.2253 $[M+H]^+$ (cald. 460.2255 for $C_{26}H_{34}ClNO_4$). The IR spectrum of **1** featured typical absorption bands for conjugated ketone (1643 cm^{-1}). The ^{13}C-*J* modulated NMR spectrum recorded in CD_3OD revealed the resonance of 26 atoms of carbon, including 7 methyl at δ_C 23.7, 22.5, 22.5, 20.5, 20.5, 12.8, 12.2 corresponding to C18, C4′ and C5′, $COCH_3$, C16, C17, and C15, respectively, 3 methylenes (C1′, C2′, and C14 at δ_C 53.7, 39.5, 30.8), 2 methine corresponding to C13 and C3′ at δ_C 35.6 and 26.6. Three carbonyl groups, including 2 conjugated ketonic carbonyl (C8 and C6 at δ_C 194.5 and 184.1, respectively), 1 ester carbonyl C19 at δ_C 170.7, 10 olefinic C atoms corresponding to C5 (corresponding to a chloro-substituted carbon), C4, C8a, C9, C11, C1, C10, C4a, C12 and C3 at δ_C 100.6, 111.4, 115.6, 116.5, 133.4, 143.0, 145.4, 146.2, 148.1, 149.9, 1 oxygenated carbon C7 at δ_C 86.3 was also depicted (Table 1). The ^1H NMR spectra revealed the presence of the 7 methyl (H15, H4′, and H5′, H16, H18, H17, $COCH_3$ at δ_H 0.87, 0.95, 0.95, 1.01, 1.44, 1.88, 2.07, respectively) and 5 olefinic protons (δ_H 5.75, 6.33, 7.02, 7.08, 7.93 corresponding to H12, H9, H4, H10, and H1) (Table 1).

The ^1H-^1H COSY spectrum of **1** highlighted the presence of two main spin-coupling systems shown in bold lines (Figure 2). The first one included the 2 olefinic methines, H9 and H10, as well as the methine H12 and H13, the methylene H14, along with the three methyl H15, H16, and H17 indicating the presence of a 3, 5-dimethyl-1,3-heptadiene moiety as a side chain. The second spin coupling system included the two methylene H1′ and H2′, the methine H3′ as well as the two methyl H5′ and H4′.

Key HMBC correlations from H1 to C3, C4a, C8, and C8a, as well as HMBC correlations from H4 to C4a, C5, C9, and C8a, from H18 to C6, and C8, indicated the presence of an isoquinoline 6,8 (*2H*, *7H*)-dione moiey characteristic of an azaphilone skeleton. HMBC correlations from H-9 to C4 and H10 to C3, along with the 3, 5-dimethyl-1,3-heptadiene moiety spin system detected in ^1H-^1H COSY spectrum allowed to connect the side chain with C3. HMBC correlation between C1′ and H1 and H3, together with the chemical shift of the methylene carbon C1′ at δ_C 53.7, suggested that C1′ is linked to an *N*-atom (Figure 2). Comparing the NMR data of compound (**1**) with penazaphilone A [8], we concluded that **1** is a sclerotioramine derivative displaying a decarboxylated leucine located at *N*2.

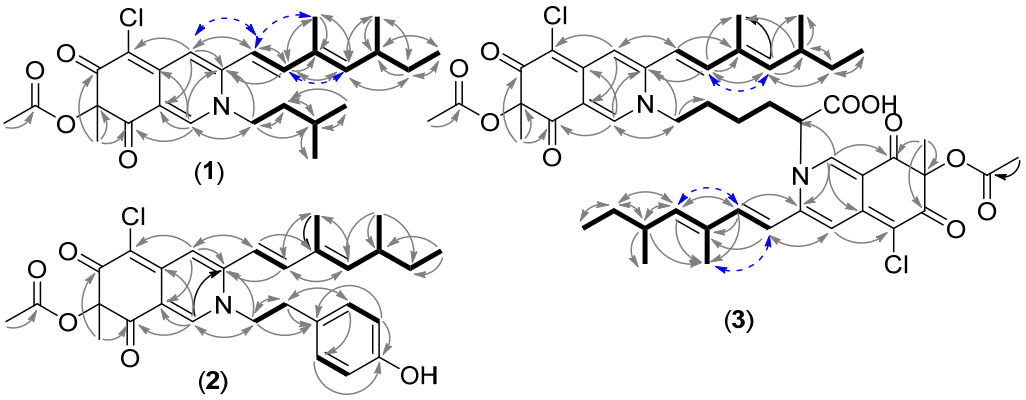

Figure 2. COSY (bold), HMBC (arrow) et NOESY (blue dashed arrow) correlations of penazaphilones J–L (**1**–**3**).

The geometry of the double bonds $\Delta^{9,10}$ and $\Delta^{11,12}$ was deduced based on the coupling constants between H9 and H10 (J = 15.5 Hz). The Overhauser effect (NOE) observed between H9 and H17, and the NOE between H10 and H12, suggesting the *E*-type $\Delta^{9,10}$ and $\Delta^{11,12}$. The observed alternate Cotton effects of **1** on the ECD spectrum were all consistent with those of penazaphilones reported in the literature [8] (Figure S7). Thus, the absolute configuration was assigned *7S*, *13S* accordingly, and compound (**1**) was thus assigned as penazaphilone J.

Compound (**2**) was obtained as a red amorphous powder and assigned a molecular formula of $C_{29}H_{32}ClNO_5$ based on the HRESIMS peak at m/z 510.2057 $[M+H]^+$. Comparison of ^{1}H NMR spectra (Table 1) of compounds **1** and **2** showed that both compounds share the same structural features, except the presence of additional aromatic signals at δ_H 6.66 and 6.96, along with the absence of a dimethyl moiety. The ^{13}C and HSQC spectra revealed the presence of 4 aromatic carbons along with a hydroxy phenol at 156.3 and a quaternary carbon at δ_C 126.7, suggesting thus the presence of a phenol on the aminated side chain. This was supported by the ^{1}H-^{1}H COSY correlations between the aromatic methine groups H4′ and H5′ and between H1′ and H2′ (Figure 3). HMBC correlations between H2′ and C3′, C4′ as well as HMBC correlations between H1′, C2′ and C3′ confirmed the presence of a 4-ethyl phenol moiety. Finally, the HMBC correlation of H1′ with C1 and C4, along with the chemical shift of H1′ at δ_H 4.25, confirmed the presence of the 4-ethyl phenol side chain at N-2.

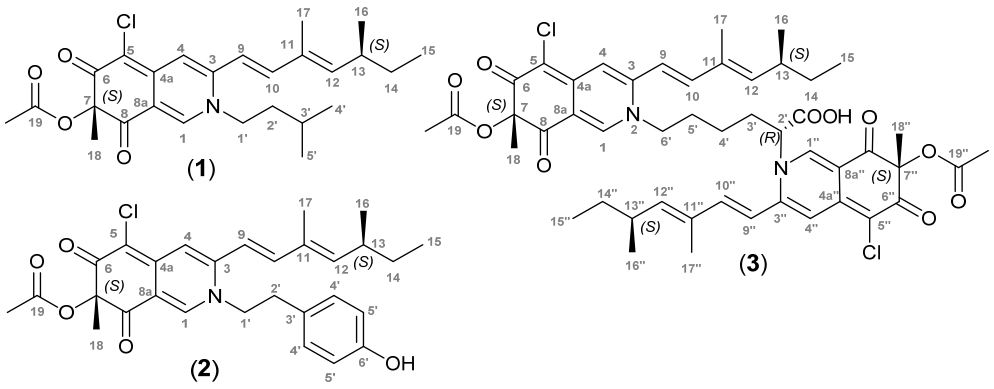

Figure 3. Structures of penazaphilones **J**–**L** (**1**–**3**).

The observed alternate Cotton effects of **2** on the ECD spectrum were all consistent with those of penazaphilones reported in the literature [8] (Figure S15). Thus, the absolute configuration was assigned *7S*, *13S* accordingly, and compound (**2**) was thus assigned as penazaphilone K.

Compound (**3**) was obtained as a red amorphous powder and assigned a molecular formula of $C_{48}H_{56}Cl_2N_2O_{10}$ based on the HRESIMS peak at *m/z* 891.3401 $[M+H]^+$, indicating 21 unsaturation degrees and suggesting a dimer compound. This compound was consistent with the node at *m/z*: 446.1716 $[M+2H]^{2+}$ observed on the molecular networking. The IR spectrum of **3** featured typical absorption bands for alcohol (3437 cm^{-1}), conjugated ketone (1703 cm^{-1}), alkene (1587 cm^{-1}), and aromatic amine (1252 cm^{-1}). The UV spectrum displayed an absorption maximum of 371 nm. The ^1H NMR and ^{13}C NMR spectra were identified to have the same planar structures as the sclerotionamine dimer [6,8].

Indeed, the ^1H NMR of **3**, along with the HSQC experiment, showed the presence of 10 methyl groups δ_H 0.87/0.86, 0.98/1.00, 1.42, 1.44, 1.82, 2.06/2.07 corresponding to, respectively, H15 and H15″, H16 and H16″, H18″, H18, H17 and H17″, and 2 $COCH_3$ and 10 olefinic protons δ_H 5.68, 5.76, 6.23, 6.24, 6.88, 6.90, 6.99, 7.03, 7.86, 7.88 corresponding to, respectively, H12″, H12, H9″, H9, H4″, H10″, H4, H10, H1″, and H1 (Table 1). From the ^{13}C NMR signals recognized as carbonyl groups were, 4 conjugated ketonic carbonyl corresponding to C6, C6″, C8″, C8 at δ_C 184.2, 184.7, 194.1, 194.4, respectively, 2 ester carbonyl corresponding to C19 and C19″ at δ_C 170.7 and 170.8, respectively, 1 carboxyl corresponding to C1′ at δ_C 171.0, 20 olefinic carbons corresponding to C5, C5″, C4, C4″, C8a, C8a″, C9, C9″, C11, C11″, C1″, C1, C4a″, C10, C10″, C4a, C12″,C12, C3, C3″ at δ_C 100.8, 102.1, 111.1, 111.8, 115.5, 115.7, 116.3, 116.7, 133.4, 133.4, 140.4, 143.1, 145.3, 145.5, 145.9, 146.2, 148.0, 148.4, 149.9, and 151.0, 2 oxygenated C-atom at δ_C 86.2 and 86.2 corresponding to C7 and C7″, 3 methine groups δ_C 35.6, 35.6, 63.7 corresponding to C13, C13″ and C2′, 6 methylene δ_C 23.2, 30.1, 30.8, 30.8, 31.9, 54.5 corresponding to, respectively, C4′, C5′, C14, C14″, C3′, C6′, and 10 methyl δ_C 12.3, 12.3, 12.8, 12.9, 20.5, 20.5, 20.5, 20.5, 23.7, 23.7 corresponding to C15, C15″, C17, C17″, C16, C16″ along with the 2 $COCH_3$, C18 and C18″. The ^1H-^1H COSY correlations allowed us to define a spin system common to each monomer and corresponding to a 3, 5-dimethyl-1,3-heptadiene moiety along with a second one, including the methylene groups H-6′, H5′, H4′, H3′ and the methine H2′ (Figure 3). Key HMBC correlations between H1″ and C3″, C4a″, C8″, between H18″ and C7″, C6″ C8″, between H4″ and C5″, along with HMBC correlations from H1 to C3, C4a, and C8, and between H18 and C7, C6 and C8, along with HMBC correlations between H4 and C5 indicated the presence of 2 isoquinoline-6,8-dione moieties, typic of the azaphilone core. HMBC correlations of H4″ with C9″ and H4 with C9 were consistent with the presence of two sclerotioramines moiety. The two dimers were linked together by the side chain defined previously on the ^1H-^1H COSY spectrum. Indeed, the HMBC correlations between H1″ and C2′ and between H1 and C6′ indicated that the side chain was linked at the N2″ and N2 atoms. This was consistent with the chemical shift of the H2′ and H6′. In addition, the chemical formula of the molecule combined with the presence of a methine H2′ allowed the carboxylic group to be placed at C2′ (Figure 3). The absolute configuration of **3** was also determined as 2R, *7S*, *7″S*, *13S*, *13″S* as both experimental and calculated ECD spectra nicely looked alike (Figure S23). The compound (**3**) was thus named penazaphilone L.

Table 1. NMR Table 1H and ^{13}C of penazaphilones J-L (**1**–**3**) (600 MHz).

	(1) [a]			**(2)** [b]			**(3)** [a]		
Pos.	δ_H	**Mult. J (Hz)**	δ_C	δ_H	**Mult. J (Hz)**	δ_C	δ_H	**Mult. J (Hz)**	δ_C
1	7.93	(s)	143.0	7.99	(s)	142.7	7.88	(s)	143.1
2	-	-	-	-	-	-	-	-	-
3	-	-	149.9	-	-	149.2	-	-	149.9
4	7.02	(s)	111.4	6.92	(s)	109.6	6.99	(s)	111.1
5	-	-	100.6	-	-	99.0	-	-	100.8
6	-	-	184.1	-	-	182.2	-	-	184.2
7	-	-	86.3	-	-	84.9	-	-	86.2
8	-	-	194.5	-	-	192.9	-	-	194.4
9	6.33	(d) 15.5	116.5	6.39	(d) 15.5	116.1	6.24	(d) 15.5	116.3

Table 1. *Cont.*

	(1) [a]			(2) [b]			(3) [a]		
Pos.	**δ_H**	**Mult. J (Hz)**	**δ_C**	**δ_H**	**Mult. J (Hz)**	**δ_C**	**δ_H**	**Mult. J (Hz)**	**δ_C**
10	7.08	(dd) 15.5; 0.8	145.4	7.09	(d) 15.4	143.8	7.03	(d) 14.8	145.5
11	-	-	133.4	-	-	132.3	-	-	133.4
12	5.75	(d) 9.7	148.1	5.85	(d) 9.7	146.5	5.76	(d) 9.7	148.4
13	2.53	(m)	35.6	2.48	(m)	34.3	2.50	(m)	35.6
14	1.45 1.32	(m)	30.8	1.43 1.30	(m)	29.5	1.43 1.31	(m)	30.8
15	0.87	(t) 7.4	12.2	0.85	(t) 7.4	11.8	0.87/0.86 *	(t) 6.3	12.3
16	1.01	(d) 6.7	20.5	0.98	(d) 6.6	20.2	1.00/0.98 *	(d) 6.7	20.5
17	1.88	(d) 1.2	12.8	1.86	(d) 1.2	12.4	1.82	(m)	12.8
18	1.44	(s)	23.7	1.37	(s)	23.1	1.44	(s)	23.7
4a	-	-	146.2	-	-	144.5	-	-	146.2
8a	-	-	115.6	-	-	113.6	-	-	115.5
4a″	-	-	-	-	-	-	-	-	145.3
8a″	-	-	-	-	-	-	-	-	115.7
1′	3.99	(m)	53.7	4.37 4.25	(ddd) 5.6; 8.2; 14.5 m	54.8	-	-	171.0
2′	1.64	(m)	39.5	2.86 2.82	(ddd) 5.6; 8.2; 14.5 m	34.7	4.95	(m)	63.7
3′	1.66	(m)	26.6	-	-	126.7	2.27 2.05	(m)	31.9
4′	0.95	(d) 6.3	22.5	6.96	(d) 8.5	129.9	1.36 1.31	(m)	23.2
5′	0.95	(d) 6.3	22.5	6.66	(d) 8.5	115.4	1.71	(m)	30.1
6′	-	-	-	-	-	156.3	3.93	(m)	54.5
1″	-	-	-	-	-	-	7.86	(s)	140.4
2″	-	-	-	-	-	-	-	-	-
3″	-	-	-	-	-	-	-	-	151.0
4″	-	-	-	-	-	-	6.88	(s)	111.8
5″	-	-	-	-	-	-	-	-	102.1
6″	-	-	-	-	-	-	-	-	184.7
7″	-	-	-	-	-	-	-	-	86.2
8″	-	-	-	-	-	-	-	-	194.1
9″	-	-	-	-	-	-	6.23	(d) 15.4	116.7
10″	-	-	-	-	-	-	6.90	(d) 15.3	145.9
11″	-	-	-	-	-	-	-	-	133.4
12″	-	-	-	-	-	-	5.68	(d) 9.7	148.0
13″	-	-	-	-	-	-	2.50	(m)	35.6
14″	-	-	-	-	-	-	1.41 1.30	(m)	30.8
15″	-	-	-	-	-	-	0.87/0.86 *	(t) 7.4	12.3
16″	-	-	-	-	-	-	1.00/0.98 *	(d) 6.6	20.5
17″	-	-	-	-	-	-	1.82	(m)	12.9
18″	-	-	-	-	-	-	1.42	(s)	23.7
$OCOCH_3$	2.07	(s)	20.5	2.06	(s)	20.1	2.06/2.07 *	(s)	20.5
$OCOCH_3$	-	-	-	-	-	-	2.06/2.07 *	(s)	20.5
19	-	-	170.7	-	-	169.1	-	-	170.7
19″	-	-	-	-	-	-	-	-	170.8

[a] CD_3CN, [b] DMSO-d_6, * signals could not be unambiguously assigned.

Penazaphilones J-L isolated in this framework did not display cytotoxicity at 100 µg/mL against various cell lines, including adenocarcinomic human alveolar basal epithelial, human bronchial epithelial, and human colon epithelial cell lines. It is noteworthy that no antimicrobial activity was observed for penazaphilones J-L against the methicillin-

resistant clinical strain of *S. aureus* N315 and the multidrug-resistant clinical strain of *P. aeruginosa*, PAH.

4. Discussion and Conclusions

By 2024, it is expected that the world color market used in the food industry will reach approximately USD 5.7 billion [18], and the contribution of the global food pigment market is projected to reach 1271.4 million USD by 2025. Unfortunately, the basic science and industry still have not overcome the high cost and low availability of natural pigments. Therefore, the demand for naturally produced biopigments will continue to rise. Microbial pigments in comparison with other natural pigments have several advantages, including an ease of scaling up and harvest, and the fact that they are not subjected to nature vagaries. Fungi are thus alternate sources of naturally derived, stable, and low-cost pigments for food industry applications [19]. One of the most promising classes of fungal pigments in research as industrial pigments are azaphilones, compounds that stand out for their yellow, orange, and red colors [5]. Azaphilones are fungal polyketides containing a highly oxygenated pyranoquinone bicyclic core and produced by numerous species of ascomyceteous and basidiomyceteous [5]. Azaphilones research is extremely important, with abundant literature. For instance, more than 600 new azaphilone derivatives displaying a wide scope of biological activities have been reported [5]. Orange azaphilones generally display a pyran oxygen-containing heterocycle, which is susceptible to aminophilic reactions with peptides, nucleic acids, or proteins. This exchange of oxygen for nitrogen changes the absorption of the pigment from orange to red and may alter its biological properties [20]. For instance, the readiness of fungi-derived red colorants for use in the food industry was discussed recently in an interesting paper by Dufossé [21].

Molecular network (MN) is a method that exploits the assumption that structurally related molecules produce similar fragmentation patterns; therefore, they should be related within a network [22]. In MN, MS/MS data are represented in a graphical form, where each node represents an ion with an associated fragmentation spectrum. The edge among the nodes represents similarities of the MS/MS spectra. Unknown but structurally related molecules can thus be highlighted, and successful dereplication can be obtained [22]. Identification of compounds can also be achieved thanks to the numerous natural products database present in the GNPS platform. A molecular network can thus be an efficient method to detect the presence of new azaphilones among complex fungal crude extract.

Herein, MN mapping of crude extract of *P. hirayamae* was performed and led to the detection of known alkaloids azaphilones such as penazaphilone D, penazaphilone F, isochromophilone VI and sclerketide E as well as new azaphilones belonging to the same cluster. These azaphilones were specifically sought by MS-guided isolation and led to the identification of three new compounds related to penazaphilone compounds named penazaphilones J-L. These compounds were fully described, and their absolute configuration was performed by ECD. To date, only nine penazaphilones have been previously reported [8]. Interestingly, most of them are devoid of cytotoxicity but display potent antimicrobial activities [23]. Penazaphilones J-L isolated in this framework did not display any cytotoxicity at 100 µg/mL on three different human cell lines used, as well as no antimicrobial on the bacterial strains tested. This study suggested thus that penazaphilones J-L may be potential fungal bio-pigments, and further investigation in the future would be necessary to consider their potential industrial development.

Furthermore, unlike *Monascus* species, which are not allowed to use azaphilones as food dyes in the USA and European countries due to the presence of co-production of toxic metabolites [24], no toxins were identified from the crude extract of *P. hirayamae* by MN. Therefore, this result suggests that *P. hirayamae* could be a potentially safe and promising fungal cell factory for the production of natural polyketide food colors.

Supplementary Materials: The following supporting information can be downloaded at: https://www.mdpi.com/article/10.3390/colorants2010003/s1. Figure S1: Full molecular network of *P. hirayamae* crude extract. Cluster or azaphilones is highlighted in yellow (known azaphilones) and green (new azaphilones). Diamond indicated azaphilones identified in the GNPS database and red square those identified, thanks to Sirius 5.5.5.; Figure S2: ^{1}H NMR (600 MHz, CD_3CN) of penazaphilone J; Figure S3: 1D NMR (600 MHz, CD_3CN) DEPT Q of penazaphilone J; Figure S4: 2D NMR (600 MHz, CD3CN) COSY of penazaphilone J; Figure S5: 2D NMR NOESY (600 MHz, CD_3CN) of penazaphilone J; Figure S6: 2D NMR (600 MHz, CD_3CN) HMBC of penazaphilone J; Figure S7: Comparison of the experimental ECD spectrum of 1 and calculated ECD spectrum for the (7S, 13S) stereoisomer; Figure S8: Absorption and emission spectra of penazaphilone J; Figure S9: 1H 1D NMR (600 MHz, DMSO-d_6) penazaphilone K; Figure S10: 1D NMR DEPT Q (600 MHz, DMSO-d_6) of penazaphilone K; Figure S11: 2D NMR COSY (600 MHz, DMSO-d_6) of penazaphilone K; Figure S12: 2D NMR NOESY (600 MHz, DMSO-*d6*) of penazaphilone K. Figure S13 2D NMR HSQC (600 MHz, DMSO-d_6) penazaphilone K; Figure S14: 2D NMR HMBC (600 MHz, DMSO-d_6) penazaphilone K; Figure S15: Comparison of the experimental ECD spectrum of 2 and calculated ECD spectrum for the (7S, 13S) stereoisomer; Figure S16: Absorption and emission spectra of penazaphilone K; Figure S17: 1D 1H NMR (600MHz, CD_3CN) of penazaphilone L; Figure S18: 1D NMR DEPTQ (600 MHz, CD_3CN) of penazaphilone L; Figure S19: 2D NMR COSY (600 MHz, CD_3CN) of penazaphilone L; Figure S20: 2D NMR NOESY (600 MHz, CD_3CN) of penazaphilone L; Figure S21: 2D NMR HSQC (600 MHz, CD_3CN) of penazaphilone L; Figure S22: 2D NMR HMBC (600 MHz, CD_3CN) of penazaphilone L; Figure S23: Comparison of the experimental ECD spectrum of 1 and calculated ECD spectrum for the (2*R*, 7*S*, 7″*S*, 13*S*, 13*S*″) stereoisomer. Figure S24 Absorption and emission spectra of penazaphilone L.

Author Contributions: Conceptualization, S.P. and X.F.; methodology, V.F, and C.P.; data analysis: A.E., T.M., S.P., X.F., C.P., G.G.-J., E.P., A.N. and V.F.; writing—original draft preparation, S.P. and X.F.; supervision, S.P. and X.F. All authors have read and agreed to the published version of the manuscript.

Funding: This work was partially supported by Normandie Université (NU), the Région Normandie, the Centre National de la Recherche Scientifique (CNRS) through the 80/Prime call and financial support to C.P., Université de Rouen Normandie (URN), INSA Rouen Normandie, Innovation Chimie Carnot (I2C), Labex SynOrg (ANR-11-LABX-0029) through financial support to V.F. and the graduate school for research XL-Chem (ANR-18-EURE-0020 XL CHEM).

Institutional Review Board Statement: Not applicable.

Informed Consent Statement: Not applicable.

Data Availability Statement: Not applicable.

Conflicts of Interest: The authors declare no conflict of interest.

References

1. Novais, C.; Molina, A.K.; Abreu, R.M.V.; Santo-Buelga, C.; Ferreira, I.; Pereira, C.; Barros, L. Natural Food Colorants and Preservatives: A Review, a Demand, and a Challenge. *J. Agric. Food Chem.* **2022**, *70*, 2789–2805. [CrossRef] [PubMed]
2. Wild, D.; Toth, G.; Humpf, H.U. New monascus metabolites with a pyridine structure in red fermented rice. *J. Agric. Food Chem.* **2003**, *51*, 5493–5496. [CrossRef] [PubMed]
3. Gao, J.M.; Yang, S.X.; Qin, J.C. Azaphilones: Chemistry and biology. *Chem. Rev.* **2013**, *113*, 4755–4811. [CrossRef] [PubMed]
4. Chen, W.; Feng, Y.; Molnar, I.; Chen, F. Nature and nurture: Confluence of pathway determinism with metabolic and chemical serendipity diversifies *Monascus* azaphilone pigments. *Nat. Prod. Rep.* **2019**, *36*, 561–572. [CrossRef] [PubMed]
5. Pavesi, C.; Flon, V.; Mann, S.; Leleu, S.; Prado, S.; Franck, X. Biosynthesis of azaphilones: A review. *Nat. Prod. Rep.* **2021**, *38*, 1058–1071. [CrossRef]
6. Li, J.; Li, Z.; Chen, T.; Ye, G.; Qiu, L.; Long, Y. New azaphilones from mangrove endophytic fungus *Penicillium sclerotiorin* SCNU-F0040. *Nat. Prod. Res.* **2021**, *37*, 296–304. [CrossRef]
7. Arai, N.; Shiomi, K.; Tomoda, H.; Tabata, N.; Yang, D.J.; Masuma, R.; Kawakubo, T.; Omura, S. Isochromophilones III-VI, inhibitors of acyl-CoA:cholesterol acyltransferase produced by *Penicillium multicolor* FO-3216. *J. Antibiot.* **1995**, *48*, 696–702. [CrossRef]
8. Tang, J.L.; Zhou, Z.Y.; Yang, T.; Yao, C.; Wu, L.W.; Li, G.Y. Azaphilone Alkaloids with Anti-inflammatory Activity from Fungus *Penicillium sclerotiorum* cib-411. *J. Agric. Food Chem.* **2019**, *67*, 2175–2182. [CrossRef]
9. Frisch, M.J.; Trucks, G.W.; Schlegel, H.B.; Scuseria, G.E.; Robb, M.A.; Cheeseman, J.R.; Scalmani, G.; Barone, V.; Petersson, G.A.; Nakatsuji, H.; et al. *Gaussian 16 Rev. C.01*; Gaussian Inc.: Wallingford, CT, USA, 2016.

10. Dillard, C.; Borde, C.; Mohammad, A.; Puchois, V.; Jourdren, L.; Larsen, A.K.; Sabbah, M.; Maréchal, V.; Escargueil, A.E.; Pramil, E. Expression Pattern of Purinergic Signaling Components in Colorectal Cancer Cells and Differential Cellular Outcomes Induced by Extracellular ATP and Adenosine. *Int. J. Mol. Sci.* **2021**, *22*, 11472. [CrossRef]
11. Le Gall, T.; Berchel, M.; Le Hir, S.; Fraix, A.; Salaün, J.Y.; Férec, C.; Lehn, P.; Jaffrès, P.A.; Montier, T. Arsonium-containing lipophosphoramides, poly-functional nano-carriers for simultaneous antibacterial action and eukaryotic cell transfection. *Adv. Healthc. Mater.* **2013**, *2*, 1513–1524. [CrossRef]
12. Youf, R.; Nasir, A.; Müller, M.; Thétiot, F.; Haute, T.; Ghanem, R.; Jonas, U.; Schönherr, H.; Lemercier, G.; Montier, T.; et al. Ruthenium(II) Polypyridyl Complexes for Antimicrobial Photodynamic Therapy: Prospects for Application in Cystic Fibrosis Lung Airways. *Pharmaceutics* **2022**, *14*, 1664. [CrossRef] [PubMed]
13. Le Gall, T.; Lemercier, G.; Chevreux, S.; Tücking, K.S.; Ravel, J.; Thétiot, F.; Jonas, U.; Schönherr, H.; Montier, T. Ruthenium(II) Polypyridyl Complexes as Photosensitizers for Antibacterial Photodynamic Therapy: A Structure-Activity Study on Clinical Bacterial Strains. *ChemMedChem* **2018**, *13*, 2229–2239. [CrossRef] [PubMed]
14. Udagawa, S. Penicillium hirayamae. *J. Agric. Sci. Tokyo Nogyo Daigaku.* **1959**, *5*, 6.
15. Udagawa, S. (-)-Sclerotiorin, A Major Metabolite of *Penicillium hirayamae* Udagawa. *Chem. Pharm. Bull.* **1963**, *11*, 366–367. [CrossRef]
16. Gray, R.W.; Whalley, W.B. The chemistry of fungi. Part LXIII. Rubrorotiorin, a metabolite of *Penicillium hirayamae* Udagawa. *J. Chem. Soc. C* **1971**, *21*, 3575–3577. [CrossRef] [PubMed]
17. Arndt, R.R.; Holzapfel, C.W.; Ferreira, N.P.; Marsh, J.J. The structure and biogenesis of desoxyverrucarin E, a metabolite of *Eupenicillium hirayamae*. *Phytochemistry* **1974**, *13*, 1865–1870. [CrossRef]
18. Food Color Market Size. *Trend Research Report*. 2023. Available online: https://www.marketresearchfuture.com/reports/food-color-market-2621 (accessed on 24 October 2022).
19. Morales-Oyervides, L.; Ruiz-Sánchez, J.P.; Oliveira, J.C.; Sousa-Gallagher, M.J.; Méndez-Zavala, A.; Giuffrida, D.; Dufossé, L.; Montañez, J. Biotechnological approaches for the production of natural colorants by *Talaromyces/Penicillium*: A review. *Biotechnol. Adv.* **2020**, *43*, 107601. [CrossRef]
20. Pimenta, L.P.S.; Gomes, D.C.; Cardoso, P.G.; Takahashi, J.A. Recent Findings in Azaphilone Pigments. *J. Fungi* **2021**, *7*, 541. [CrossRef]
21. Dufossé, L. Red colourants from filamentous fungi: Are they ready for the food industry? *J. Food Compos. Anal.* **2018**, *69*, 156–161. [CrossRef]
22. Wang, M.; Carver, J.J.; Phelan, V.V.; Sanchez, L.M.; Garg, N.; Peng, Y.; Nguyen, D.D.; Watrous, J.; Kapono, C.A.; Luzzatto-Knaan, T.; et al. Sharing and community curation of mass spectrometry data with Global Natural Products Social Molecular Networking. *Nat. Biotechnol.* **2016**, *34*, 828–837. [CrossRef]
23. Chen, C.; Tao, H.; Chen, W.; Yang, B.; Zhou, X.; Luo, X.; Liu, Y. Recent advances in the chemistry and biology of azaphilones. *RSC Adv.* **2020**, *10*, 10197–10220. [CrossRef] [PubMed]
24. Mapari, S.A.S.; Thrane, U.; Meyer, A.S. Fungal polyketide azaphilone pigments as future natural food colorants? *Trends Biotechnol.* **2010**, *28*, 300–307. [CrossRef] [PubMed]